The Effects of Impingement and Dysplasia on Stress Distributions in the Hip Joint during Sitting and Walking: A Finite Element Analysis

Salman Chegini,[1] Martin Beck,[2] Stephen J. Ferguson[1]

[1]MEM Research Center for Orthopaedic Surgery, University of Bern, Stauffacherstrasse 78, CH-3014 Bern, Switzerland, [2]Department of Orthopedic Surgery, Inselspital, University of Bern, CH-3010 Bern, Switzerland

Received 8 December 2007; accepted 26 June 2008
Published online 27 August 2008 in Wiley InterScience (www.interscience.wiley.com). DOI 10.1002/jor.20747

ABSTRACT: Soft tissue damage has been observed in hip joints with pathological geometries. Our primary goal was to study the relationship between morphological variations of the bony components of the hip and resultant stresses within the soft tissues of the joint during routine daily activities. The secondary goal was to find the range of morphological parameters in which stresses are minimized. Computational models of normal and pathological joints were developed based on variations of morphological parameters of the femoral head (Alpha angle) and acetabulum (CE angle). The Alpha angle was varied between 40° (normal joint) and 80° (cam joint). The CE angle was varied between 0° (dysplastic joint) and 40° (pincer joint). Dynamic loads and motions for walking and standing to sitting were applied to all joint configurations. Contact pressures and stresses were calculated and crosscompared to evaluate the influence of morphology. The stresses in the soft tissues depended strongly on the head and acetabular geometry. For the dysplastic joint, walking produced high acetabular rim stresses. Conversely, for impinging joints, standing-to-sitting activities that involved extensive motion were critical, inducing excessive distortion and shearing of the tissue–bone interface. Zones with high von Mises stresses corresponded with clinically observed damage zones in the acetabular cartilage and labrum. Hip joint morphological parameters that minimized were $20^\circ \leq CE \leq 30^\circ$ and alpha $\leq 50^\circ$. © 2008 Orthopaedic Research Society. Published by Wiley Periodicals, Inc. J Orthop Res 27:195–201, 2009

Keywords: hip joint; finite element; impingement; dysplasia; contact stress

Hip osteoarthritis is a multifactorial disease. Possible initiators include impaired nutrition, genetics, gender or a combination of these factors. However, the mechanical environment plays a principal role in cartilage degeneration in the joint. The internal pressure distribution within the joint is, in turn, heavily influenced by applied loads, the mechanical properties of the cartilage layers, and the anatomical conformation of the joint surfaces. The morphology of the hip varies depending on age, gender, race, and developmental changes.[1] Hip dysplasia, a congenital and developmental deformity characterized by a malorientation and a reduction of contact area between femur and acetabulum, has been proposed as the most common cause of hip OA.[2] The loss of lateral and anterior coverage of the head by the acetabulum increases contact pressure and concentrates pressure on the anterolateral edge of the acetabulum during normal activities.[3] The mechanism of degeneration in the dysplastic hip is well understood, but determining the pathogenesis for idiopathic OA remains an elusive goal. Recently, femoroacetabular impingement has been introduced as a potential initiator of hip OA.[4] The concept focuses more on motion than on axial loading, but is nevertheless a problem of morphological variations that fall outside the range of "normal" joint geometry. Although the hypothesis is supported by clinical observations, no biomechanical study has been conducted to investigate this mechanism.

The morphology of the hip is well described by selected anatomical parameters. One important parameter is acetabular coverage, defined by the center-edge (CE) angle (Fig. 1a), defined as the angle formed by the perpendicular to the intertear drop line and the line passing from the center of the femoral head to the lateral edge of the acetabulum.[5] More recently, morphological variation in the femoral head has been quantified. The Alpha (α) angle (Fig. 1b) describes the relationship between femoral head and neck anatomy and is measured as the angle between A–O and O–O′, where O is the head center, O′ is the center of the neck at the narrowest point, and A is the anterior point where the femoral head diverges from spherical.[6] For a CE angle $<20^\circ$, coverage of the femoral head by the acetabulum is insufficient, and risk of subluxation exists; this is the classical dysplastic joint. For a CE angle $>30^\circ$, overcoverage of the femoral head by the acetabular roof leads to impingement between the normal neck and the extended acetabular rim during motion; this is the pincer type joint. For the femur, deviation from the normal geometry is usually associated with alpha angles $>50^\circ$, taking the form of an aspherical protuberance at the head–neck junction that is forced against and into the rim during extreme motions; this impingement is cam type, due to the analogous mechanical principal (Fig. 1c).

The biomechanics of the hip joint have been studied using both experimental and computational methods. Experimental methods have been used to measure contact pressures inside the joint.[7–10] Computational methods have been used to calculate the contact pressure inside the hip[3,9] and have been employed to verify relationships between morphological changes and contact pressures.[3] No study has specifically examined the effect of impingement on hip biomechanics to provide information about the usefulness of current surgical procedures. Surgical treatment of the dysplastic hip involves reorientation of the acetabular roof to improve femoral coverage. Surgical treatment of femoroacetabular impingement focuses on improving the clearance for

Correspondence to: Salman Chegini (T: +41 31 631 5937; F: +41 31 631 5960; E-mail: salman.chegini@artorg.unibe.ch)

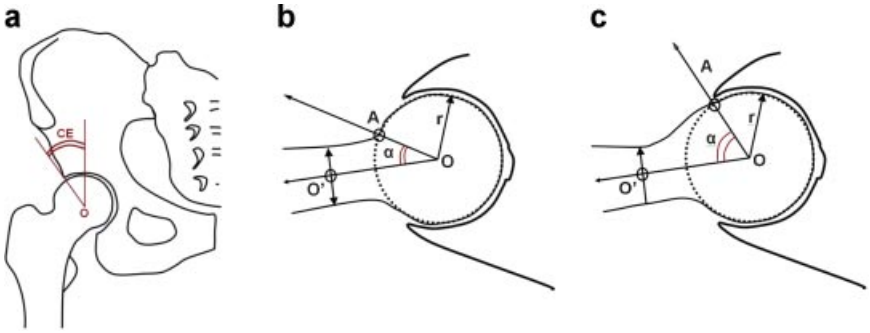

Figure 1. (a) Definition of the CE angle as an indication of femoral head coverage. (b) Definition of the alpha angle on the femoral head. (c) Alpha angle of a typical cam type joint.

hip motion and alleviating femoral abutment against the acetabular rim. Early surgical intervention for impingement, besides relieving symptoms, may decelerate the progression of the degenerative process,[4] and indeed good to excellent midterm results have been reported.[11]

To evaluate and compare the relative importance of dysplasia and femoroacetabular impingement as mechanical initiators of hip OA, it is relevant to determine the effects of geometrical variations on the stresses in the joint during normal activities. Furthermore, the potential to determine optimal CE and alpha angles for low-stress joint operation may provide appropriate guidelines for corrective surgery. Our goal was to create 3D computational models of the femoroacetabular articulation that cover a broad range of CE and alpha angles and to determine the mechanical response of the cartilage layers during simulated walking and standing-to-sitting activities. We hypothesized that femoroacetabular impingement and dysplasia result in characteristic patterns of stress and contact pressure consistent with clinically observed joint degeneration and that an optimal range of CE and alpha angles exists that minimizes contact pressures and cartilage stresses for these activities.

MATERIALS AND METHODS

Left hip joint models were developed with CE angles of 0, 10, 20, 30, and 40° and alpha angles of 40, 50, 60, 70, and 80°. The normal and pathological models were developed in CAD software (Solidworks 2005, Solidworks Corp., Boston, MA). Combinations of the different acetabuli and femoral heads produced a matrix of 25 different joints, ranging from a dysplastic joint to a severely impinging joint (cam, pincer, and combined cam + pincer). The principal joint morphologies are shown in Figure 2a–d, and the cross-sectional geometry of the idealized model in the coronal plane is compared with the native hip geometry in Figure 2e–f.

The femoral head cartilage was assumed to be 2 mm at the thickest point, gradually reducing to zero toward the lateral edge;[12] the acetabular cartilage had a constant thickness of 2 mm. The femoral and acetabular cartilage surfaces are known to be spherical with deviations from sphericity on the order of <100 μm.[9] Therefore, the articulating joint surfaces were modeled as portions of spherical surfaces with a common 25-mm radius. The anatomical horseshoe shape of the acetabular cartilage was taken into account, and the lateral acetabular coverage was altered by 10° step changes in CE angle, while maintaining the same medial border, to create the variety of joints. The labrum was defined based on morphological studies, such that it covered the femoral head cartilage in the unloaded condition with a triangular cross-section and a height of 7 mm from the acetabular rim to the tip.[13]

Solid models were imported to finite element software (ABAQUS 6.6, ABAQUS Germany Ltd., Aachen, Germany) and were meshed with 20-node quadratic brick elements (Fig. 2). Cartilage was modeled as an isotropic, linear elastic material with $E = 12$ MPa, and $\upsilon = 0.45$.[14] Cartilage is a biphasic material with time-dependent mechanical behavior. However, the loading frequency for normal activities like

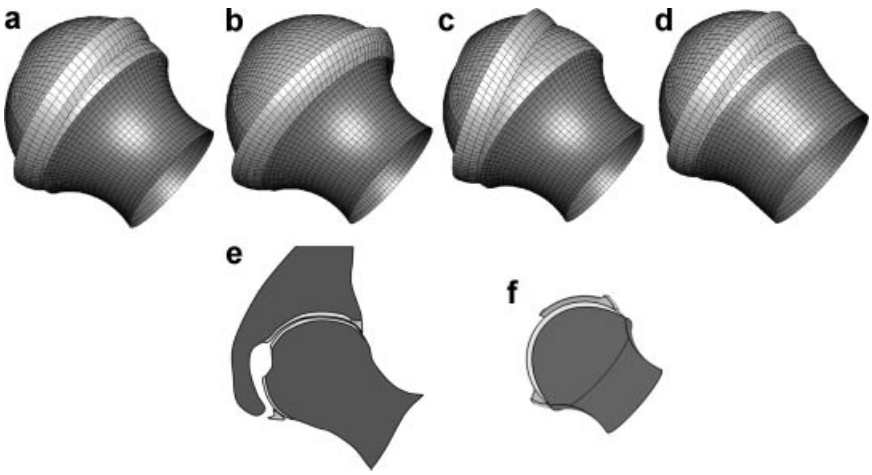

Figure 2. (a) Normal joint. (b) Pincer type joint. (c) Dysplastic joint. (d) Cam-type joint. Comparison of sectional geometry of a natural joint (e), traced from cryosections, with the CAD-generated model geometry (f).

walking and stance to sit are on the order of 1 Hz; therefore, time-dependent behavior can be neglected.[15] The material properties of labral tissue were extracted from the toe region of tensile tests and set to be $E = 20$ MPa, and $\upsilon = 0.4$.[16] A surface-based, finite sliding contact was defined between the femoral cartilage, as master surface, and acetabular cartilage and labrum as slave surfaces, with an assumed frictionless interaction. The bony structures of the acetabulum and femur were modeled as rigid bodies, as pilot analyses showed no differences in predicted cartilage stresses for models with rigid and elastic bone structures. The pilot analysis was a simplified, axisymmetric model of the acetabular socket and surrounding bone, with a cortical shell thickness of 1.5 mm, elastic modulus of $E = 20$ GPa, and isotropic and homogeneous trabecular bone of $E = 100$ Mpa.

Stress and pressure in the joint depends on the patterns of load and motions acting on the joint. The most frequent loading cases during daily activities are walking and the transition from standing to sitting. These two activities cover a broad range of loading, in that standing to sitting is accomplished over an extreme flexion range, while high loads are applied over small rotations for walking. Time dependent loads and motions for standing to sitting and walking were obtained from in vivo experiments.[17] In vivo force and motion data were combined into a synchronized input file. For the simulation, the acetabulum was fixed and 3D motion data were applied as a prescribed rotation about the femoral head center (θ_x, θ_y, θ_z) with unconstrained translations, and the corresponding joint reaction force vector was simultaneously applied (F_x, F_y, F_z) in a coordinate system with the *X, Y,* and *Z* axes being lateral–medial, posterior–anterior, and vertical upward, respectively, originating from the head center. The applied force on the head center was balanced by the integrated vector sum of all contact pressures, including the impinging reaction at the outer margins of the acetabulum. Walking motion was simulated from heel strike through to maximum load during stance. The body weight (BW) for the walking case was 836 N, and the maximum force during stance was 230% BW. In stance to sitting, the BW was the same, and the maximum load was 156% BW. Stand to sit was used instead of sit to stand to have an identical initial condition (upright standing) as the walking simulation.

RESULTS

Contact pressure and von Mises stresses were calculated over the full loading cycle during walking and stance to sitting for all 25 combinations of hip joint geometries. The reported stresses represent the highest magnitude stresses that occurred over the full motion cycle. During walking, this tended to coincide with the instant of maximum force, after heel strike and just prior to the contraleteral foot toeoff, while for standing to sitting, these occurred during maximum flexion and rotation, also the point of maximum force, just prior to seat contact. Peak contact pressures are presented in Table 1, and show that the contact pressure was dependent on CE and alpha angles and activity type. In normal joints ($20^\circ < \mathrm{CE} < 30^\circ$ and $\alpha < 50^\circ$), the peak contact pressure was a minimum. In a typical contact pressure profile for a dysplastic joint, focal overloading of the lateral edge of the acetabulum was observed during walking due to the shallow and vertically oriented acetabulum.

The distribution of von Mises stress, a measure of internal distortion energy in the cartilage layers, is shown in Figure 3 for the stance-to-sitting motion for all joint geometries. With a constant alpha angle, increasing the CE angle lead to higher stresses at the acetabular rim, due to abutting contact with the femoral neck and the labrum (pincer impingement). When the alpha angle was increased for a constant CE angle, an intrusion of the nonspherical portion of the head into the acetabulum resulted (cam impingement), with a consequent concentration of cartilage stresses at the anterior border of the

Table 1. The Variation In Peak Contact Pressure (Mpa) in the Acetabular Cartilage and Labrum Occurring during Standing to Sitting and Walking

Standing to sitting					
CE→	0°	10°	20°	30°	40°
Alpha↓					
40°	3.48	3.6	3.66	3.34	3.71
50°	3.48	3.6	3.69	3.36	3.64
60°	3.48	3.6	3.67	3.68	10.52
70°	3.48	3.61	3.78	7.51	16.51
80°	3.49	4.7	8.84	12.84	16.51
Walking					
CE→	0°	10°	20°	30°	40°
Alpha↓					
40°	9.92	6.08	3.55	2.35	1.81
50°	9.92	6.08	3.55	2.35	1.81
60°	9.92	6.08	3.55	2.35	1.81
70°	9.92	6.08	3.55	2.35	1.81
80°	9.92	6.08	3.55	2.35	1.81

acetabulum at maximum flexion. A typical von Mises stress profile for a cam type joint is shown in Figure 4b and compared to a clinical image of delamination of acetabular cartilage at the same location (Fig. 4a).

To visualize the changes in calculated results with morphologcial variation, the peak von Mises stresses were plotted as a function of CE and alpha angles (Figs. 5a–c). Peak von Mises stresses during walking were directly related to CE angle (Fig. 5a), such that stresses increased dramatically as the angle decreased. As the nonspherical portion of the head–neck junction does not contact the acetabular rim during walking, the alpha angle was not a determinant of joint stresses during walking. Peak von Mises stresses during standing to sitting are plotted in Figure 5b as a function of CE and alpha angles. Standing to sitting involves more extreme rotation angles, and the maximum stresses were related to changes of both angles. The highest stresses occurred for simultaneous maximum values of alpha and CE angles, which correspond to a severe case of impingement (a combination of cam and pincer type).

Combining the walking and stance to sit results into a single graph (Fig. 5c), choosing the absolute maximum peak stress from either loading dataset, showed that the dysplastic hip was predominantly susceptible to overloading, whereas the impingement hip was most sensitive to large motions. Furthermore, the minimum stresses occurred for a joint with CE and alpha angles in the normal range.

For standing to sitting, the maximum head center translation was 0.2 to 0.3 mm for most joints. The vector representing this translation for a normal joint was (0.23, 0.10, and 0.02 mm) in the defined coordinate system. For walking, the displacement of the head center exhibited a different pattern and magnitude, moving more superolaterally and even subluxating for extremely dysplastic joints. The vector representing this translation for a normal joint was (−0.42, −0.12, and 0.3 mm).

DISCUSSION

The stresses within the soft tissues (labrum and acetabular cartilage) of the hip joint during the daily activities are highly dependent on the geometry of the bony anatomy and the type of activity. For standing to sitting, increasing the alpha angle resulted in intrusion of the bony protrusion of the femoral head/neck into the acetabulum, producing high von Mises stresses in the soft tissues at the anterosuperior acetabular rim,

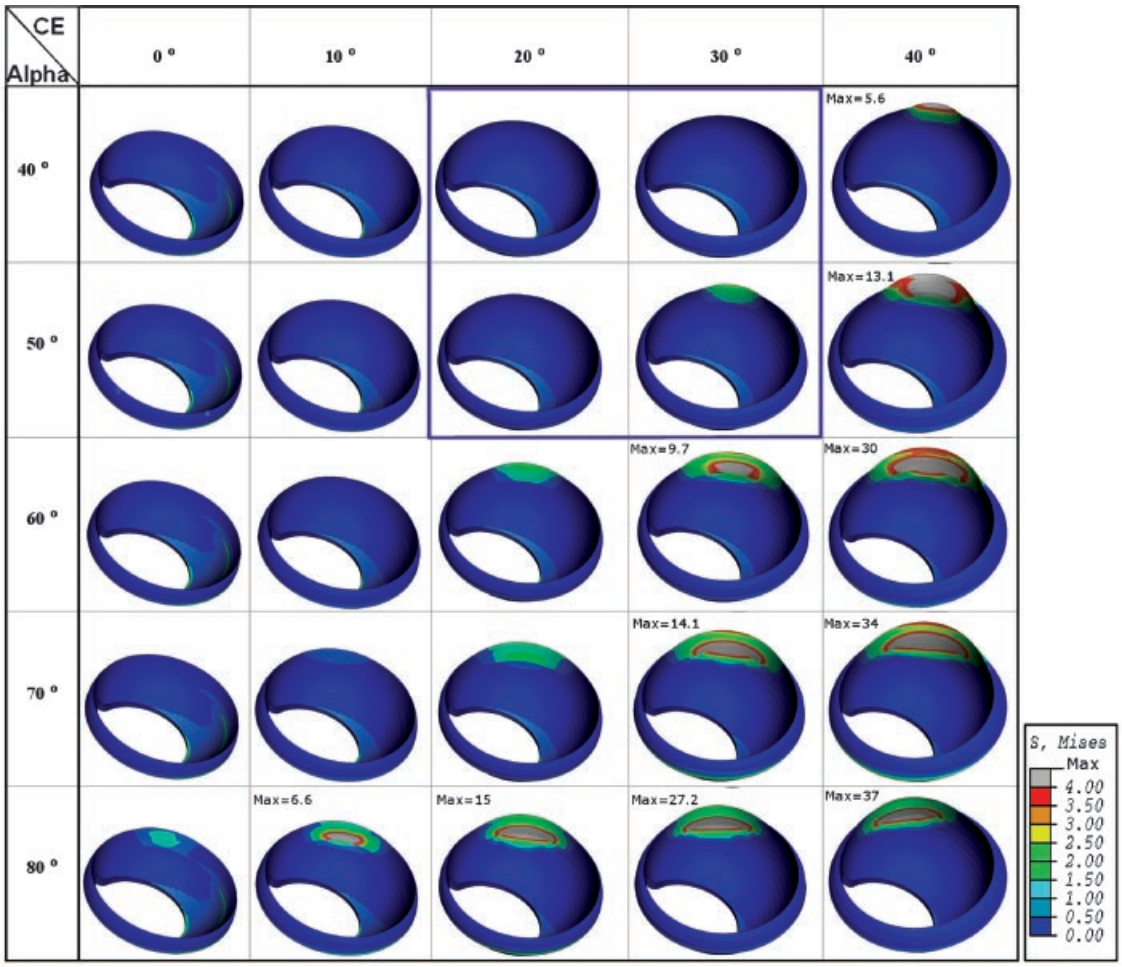

Figure 3. Distribution of von Mises stresses (MPa) within the acetabular cartilage during standing to sitting for all simulated joint geometries. The joints considered as normal are encompassed in the blue rectangle.

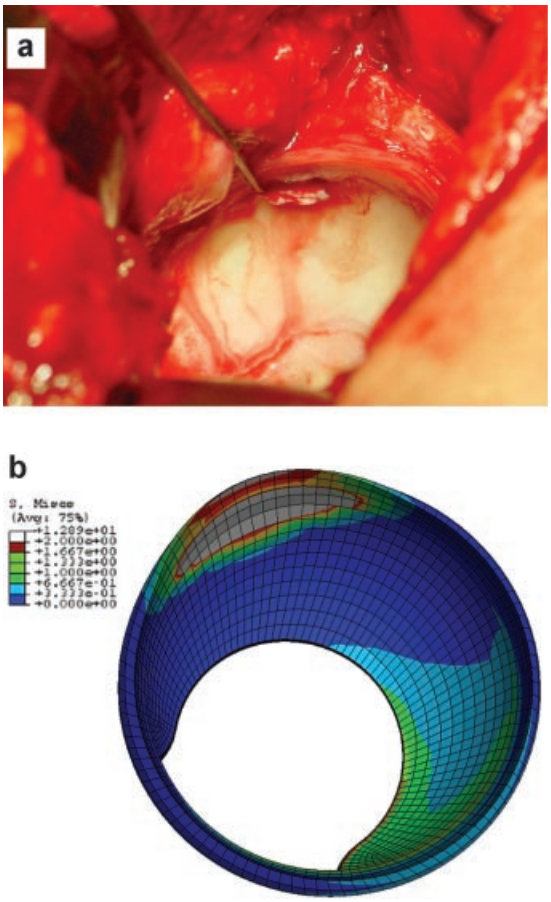

Figure 4. Damage patterns: (a) observed intraoperatively at the anterior–superior acetabular rim for a typical cam impingement, (b) von Mises stress distribution in a typical cam-type ($\alpha = 80^{\circ}$) joint for deep flexion in the standing-to-sitting motion (anterior = left).

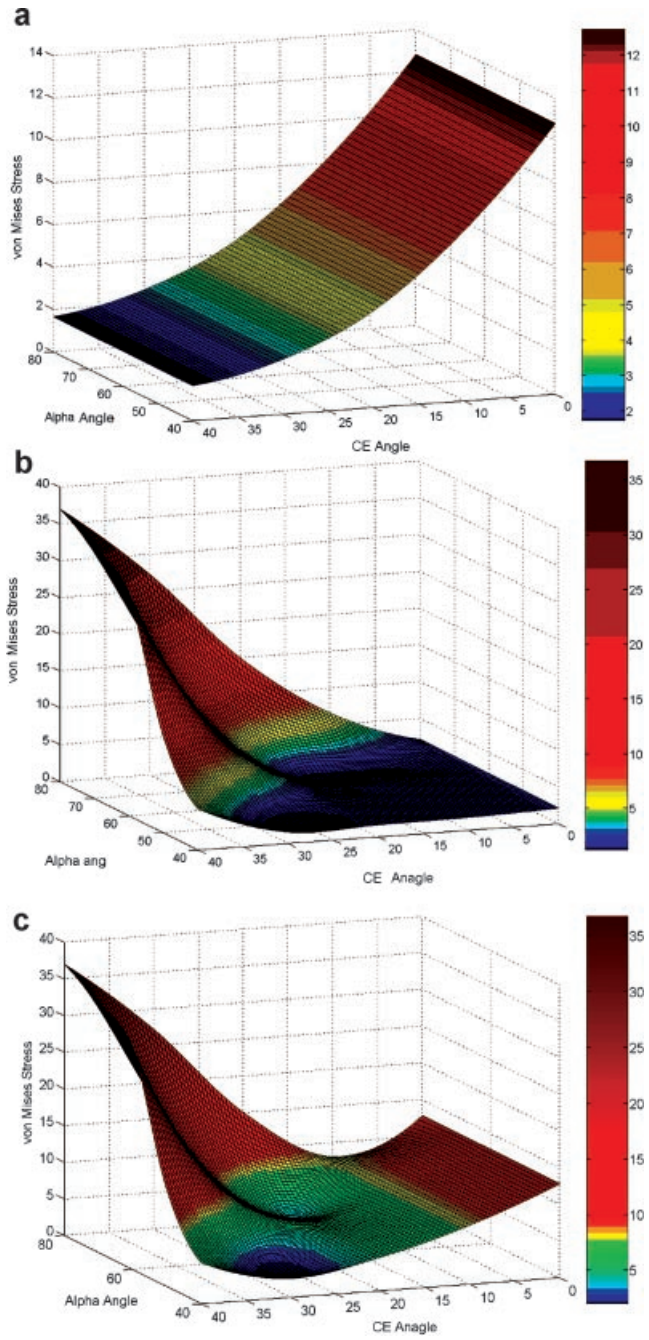

Figure 5. Variation in maximum von Mises stress in acetabular cartilage: (a) during walking for all simulated joint geometries. (b) During stance-to-sit motion for all simulated joint geometries. (c) During combined activities (walking and stance to sit combined) for all simulated joint geometries.

while increasing the CE angle resulted in impingement of the head–neck junction against the labrum, causing high stresses in the labrum and adjacent acetabular cartilage. Therefore, standing to sitting is a critical activity for impinging joints because it includes more rotation, introducing high contact pressures and soft-tissue distortion. Conversely, reducing the CE angle to $<20^{\circ}$ lead to insufficient head coverage and eventually high von Mises stresses and contact pressures in this small coverage zone for dysplastic joints, especially during walking, an activity with high loads rather than a large range of motion.

Our finite element results can be compared with previously conducted in vitro and in vivo experiments, as well as computational models. Our contact pressures were dependent on both activity (applied force and motion) and joint morphology and varied from 3.34 to 16.51 MPa during standing to sitting and 1.81 to 9.92 MPa for walking (Table 1). Experimentally measured contact pressures are inconsistent and dependent on the implemented measurement methods. Brown and Shaw[7] measured hip joint contact pressure using implanted pressure transducers in vitro, and found a pressure of 8.8 MPa for an applied load of 2700 N. They also compared previous measurements and reported values that ranged from 3.32 MPa during 5 BW[18] to 11.1 MPa peak pressure during a 2250-N applied load.[19] This controversy may be due to changing the natural environment of the hip via the measurement process. In vivo measurements performed by Hodge et al.[8] using an instrumented endoprosthesis included a peak contact pressure of 5.5 MPa postoperatively during sitting to standing. Our simulation results are in the range of experimental data. Beside variations among experimental results, the simulation results could differ

from experiments due to the asphericity of the natural femoral head (on the order of 100 μm), which was not taken into account in our study. Also, cartilage material properties may vary from patient to patient, while the same material properties were used for all simulations.

On the computational side, Genda et al.[3] reported peak contact pressure as a function of CE angle. The maximum value with CE = 18° was 3.5 MPa, which is quite consistent with our results (3.5 MPa for CE = 20°). The recent finite element analysis conducted by Bachtar et al.[20] reported the contact pressure as 5.5 MPa, not mentioning the effect of acetabular geometry. Although our results agree with previous computational models in normal joints, the range of contact pressure calculated in our study is higher (up to 16.5 MPa for severe impingement), which was not reported in previous computational models. We found no experiments reporting contact pressure in the impinging joints with which to compare our results.

Clinically in impinging joints labrum degeneration and cartilage delamination occurs in the anterior superior region of the acetabulum.[21] This pathology is mostly observed in young and active adults like football players, dancers, gymnasts, and hockey players, who tend to perform extreme hip motions, often with simultaneous heavy loading,[22] but also in normally active patients. In acetabular dysplasia, joint damage is observed at the anterosuperior area of the acetabular rim. Our findings are consistent with clinical observations and show that the damaged zone is related to high von Mises stress zones. The zone of cartilage delamination for a cam type impinging joint and the result of our simulation during sitting are consistent (Fig. 4). This may a result from substantial fiber distortion at the bone–cartilage interface, eventually leading to fatigue failure of this important connection.

Although peak von Mises stresses occurred at the same time as peak contact pressures for all hip geometries and load cases, temporal and spatial patterns varied during the motion cycle for different joint types. For normal and dysplastic hips, von Mises stress location and timing closely followed contact pressure, indicating that total joint loading is the determining factor for the internal mechanical environment. For impinging joints, contact pressure generally followed the orientation and timing of the net joint reaction force for walking and sitting to standing, but maximum von Mises stresses increased dramatically at the impingement location during sitting. Hence, motion is the dominant determinant for the internal mechanical environment in the impinging joint.

Cartilage and labral damage in early OA due to dysplasia or impingement can bring the patient to the surgeon. Current methods for surgical preservation of the hip, an action usually taken before severe OA is evident, is a resection or reorientation osteotomy.[23,24] This method tends to return the joint geometry to normal, preventing impingement or correcting dysplasia, and increasing the range of painless motion.

Clinically, only limited information exists about the normal shape of the acetabulum, and the upper normal value of the CE angle is unknown. We showed that with a CE angle between 20° to 30°, the combined high force- and motion-induced stresses are at their lowest values, so normal coverage of the hip should be within this range. Our data show that for daily activities of walking and sitting the stresses are minimum if the CE and Alpha angles are in a range of $20° \leq CE \leq 30°$ and alpha $\leq 50°$. These results could be used as in operative planning, possibly in conjunction with computer guided surgery to facilitate complex osteotomies,[25] keeping the limitations of the model in mind.

Although this model provides useful information for understanding the etiology of joint degeneration and for surgical planning, the simplifying assumptions should be considered. Cartilage is a highly structured biphasic, anisotropic material, and accounting for these properties, as well as tribological aspects, would give more detailed information about load sharing between the solid phase and interstitial synovial fluid. In this study, joint geometries were created using CAD software. Models derived directly by segmentation of imaging datasets (CT, MRI) would provide a more realistic joint geometry, although current imaging modalities lack the required resolution to directly create accurate representations of the articular surfaces. Clinical MRI offers a resolution of about 0.3 mm, which is 10 to 20% of the nominal cartilage thickness, whereas direct measurements of articular geometry reveal surface undulations an order of magnitude smaller. Directly imported articular geometry can create convergence problems in finite element simulations with contact, whereas manual correction and smoothing of segmented surfaces may deviate from the real geometry. Similarly, while patient-specific models derived from CT data allow an accurate representation of the osseous anatomy, a significant amount of manual intervention or geometry correction is required to create realistic articular surfaces.[26] Therefore, the goal of evaluating the influence of specific hip morphological variations in a parametric model is efficiently and reasonably met with CAD-defined geometry, despite the lack of patient specificity. The average loads from in vivo measurements are applied in this study, but the pattern of loading may vary for different subjects, thus, more data on the joint dependent load would be helpful to increase the accuracy of the simulation. In the absence of data from subjects with pathological joints, simulations based on normal forces and motions provide a prediction of internal joint stresses that define a lower bound for the pathological cases.

In conclusion, stresses occurring in the soft tissues of the hip joint depend on joint geometry, motion, and load. Degeneration of the dysplastic joint is likely an unavoidable consequence of normal locomotion, whereas the impinging joint is most sensitive to extreme motions. Zones with high von Mises stresses correspond with clinically observed damage zones in the acetabular cartilage and labrum. An optimal range of the hip joint

morphological parameters exists ($20^\circ \leq CE \leq 30^\circ$, and alpha $\leq 50^\circ$), whereby internal stresses and pressures are minimized, and this provides useful information for the planning of surgical resection or reorientation.

ACKNOWLEDGMENTS

Funding was provided by the Swiss National Science Foundation (NCCR CO-ME) and the Synos Foundation.

REFERENCES

1. Than P, Sillinger T, Kranicz J, et al. 2004. Radiographic parameters of the hip joint from birth to adolescence. Pediatr Radiol 34:237–244.
2. Michaeli DA, Murphy SB, Hipp JA. 1997. Comparison of predicted and measured contact pressures in normal and dysplastic hips. Med Eng Phys 19:180–186.
3. Genda E, Iwasaki N, Li G, et al. 2001. Normal hip joint contact pressure distribution in single-leg standing—effect of gender and anatomic parameters. J Biomech 34:895–905.
4. Ganz R, Parvizi J, Beck M, et al. 2003. Femoroacetabular impingement: a cause for osteoarthritis of the hip. Clin Orthop Relat Res 417:112–120.
5. Wiberg G. 1939. Studies on dysplastic acetabular and congenital subluxation of the hip joint: with special reference to the complication of osteo-arthritis. Acta Chir Scand 58: 7–38.
6. Notzli HP, Wyss TF, Stoecklin CH, et al. 2002. The contour of the femoral head-neck junction as a predictor for the risk of anterior impingement. J Bone Joint Surg Br 84:556–560.
7. Brown TD, Shaw DT. 1983. In vitro contact stress distributions in the natural human hip. J Biomech 16:373–384.
8. Hodge WA, Fijan RS, Carlson KL, et al. 1986. Contact pressures in the human hip joint measured in vivo. Proc Natl Acad Sci USA 83:2879–2883.
9. Macirowski T, Tepic S, Mann RW. 1994. Cartilage stresses in the human hip joint. J Biomech Eng 116:10–18.
10. von Eisenhart R, Adam C, Steinlechner M, et al. 1999. Quantitative determination of joint incongruity and pressure distribution during simulated gait and cartilage thickness in the human hip joint. J Orthop Res 17:532–539.
11. Beck M, Siebenrock KA, Affolter B, et al. 2004. Increased intraarticular pressure reduces blood flow to the femoral head. Clin Orthop Relat Res 424:149–152.
12. Eckstein F, Adam C, Sittek H, et al. 1997. Non-invasive determination of cartilage thickness throughout joint surfaces using magnetic resonance imaging. J Biomech 30: 285–289.
13. Won YY, Chung IH, Chung NS, Song KH. 2003. Morphological study on the acetabular labrum. Yonsei Med J 44:855–862.
14. Moglo KE, Shirazi-Adl A. 2003. On the coupling between anterior and posterior cruciate ligaments, and knee joint response under anterior femoral drawer in flexion: a finite element study. Clin Biomech 18:751–759.
15. Ateshian GA, Ellis BJ, Weiss JA. 2007. Equivalence between short-time biphasic and incompressible elastic material responses. J Biomech Eng 129:405–412.
16. Ferguson SJ, Bryant JT, Ito K. 2001. The material properties of the bovine acetabular labrum. J Orthop Res 19:887–896.
17. Bergmann G, Deuretzbacher G, Heller M, et al. 2001. Hip contact forces and gait patterns from routine activities. J Biomech 34:859–871.
18. Brinckmann P, Frobin W, Hierholzer E. 1981. Stress on the articular surface of the hip joint in healthy adults and persons with idiopathic osteoarthrosis of the hip joint. J Biomech 14:149–156.
19. Rushfeldt PD, Mann RW, Harris WH. 1981. Improved techniques for measuring in vitro the geometry and pressure distribution in the human acetabulum—I. Ultrasonic measurement of acetabular surfaces, sphericity and cartilage thickness. J Biomech 14:253–260.
20. Bachtar F, Chen X, Hisada T. 2006. Finite element contact analysis of the hip joint. Med Biol Eng Comput 44:643–651.
21. Beck M, Kalhor M, Leunig M, Ganz R. 2005. Hip morphology influences the pattern of damage to the acetabular cartilage: femoroacetabular impingement as a cause of early osteoarthritis of the hip. J Bone Joint Surg Br 87:1012–1018.
22. Bizzini M, Notzli HP, Maffiuletti NA. 2007. Femoroacetabular impingement in professional ice hockey players: a case series of 5 athletes after open surgical decompression of the hip. Am J Sports Med 35:1955–1959.
23. Lavigne M, Parvizi J, Beck M, et al. 2004. Anterior femoroacetabular impingement: part I. Techniques of joint preserving surgery. Clin Orthop Relat Res 418:61–66.
24. Siebenrock KA, Leunig M, Ganz R. 2001. Periacetabular osteotomy: the Bernese experience. Instr Course Lect 50:239–245.
25. Langlotz F, Bachler R, Berlemann U, et al. 1998. Computer assistance for pelvic osteotomies. Clin Orthop Relat Res 354:92–102.
26. Russell ME, Shivanna KH, Grosland NM, Pedersen DR. 2006. Cartilage contact pressure elevations in dysplastic hips: a chronic overload model. J Orthop Surg 3:1–6.